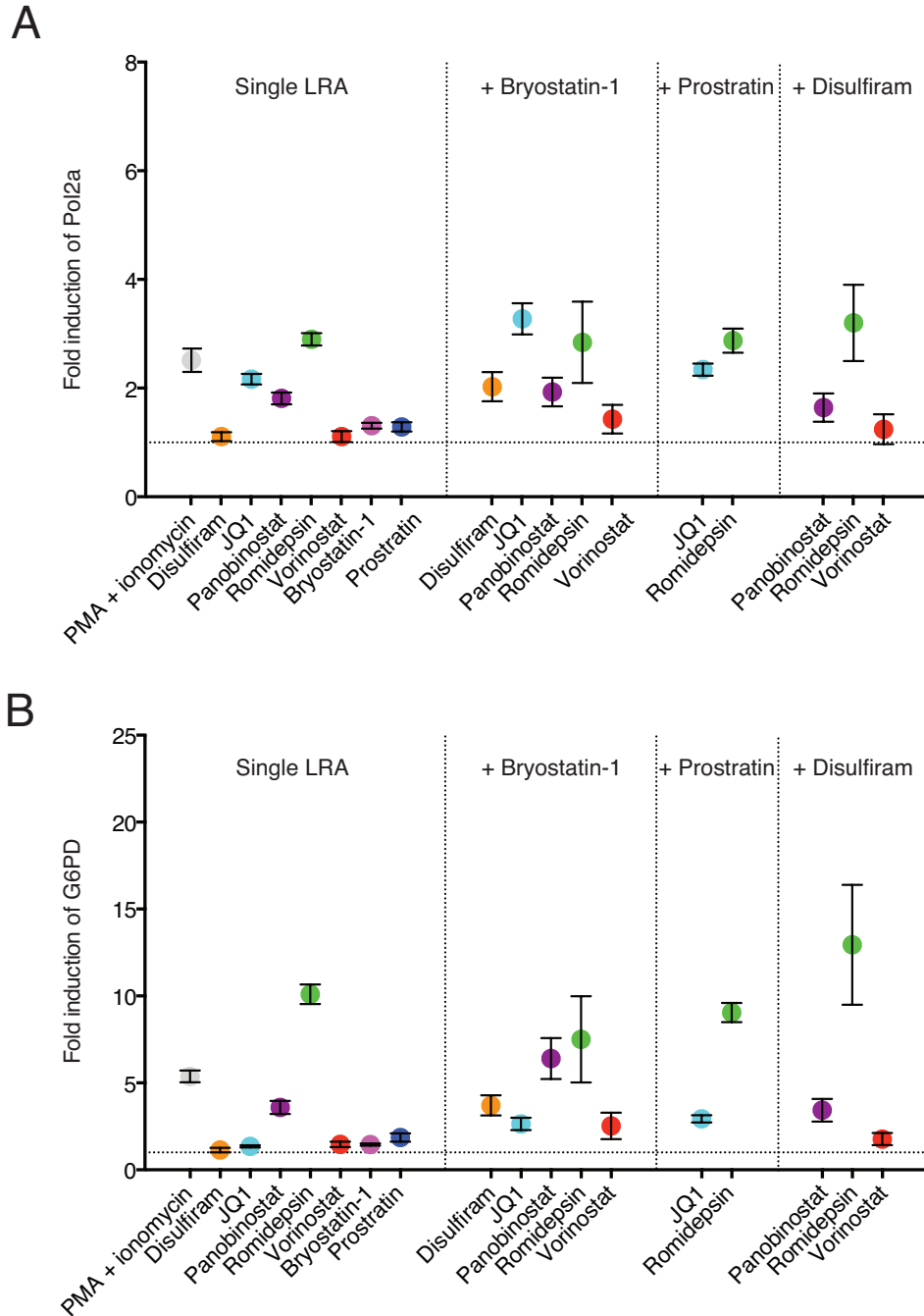**Supplementary Figure 1. LRA combinations induce intracellular HIV-1 mRNA production in rCD4s from infected individuals on ART.** Intracellular HIV-1 mRNA levels in rCD4s, obtained from infected individuals and treated ex vivo with a single LRA or a combination of two LRAs, presented as copies per million rCD4 equivalents. Numbers in parentheses in Fig. 1A indicate number of individuals used for each treatment.

Supplementary Figure 2. LRA combinations do not increase expression of endogenous housekeeping genes above that caused by a single LRA treatment. Relative expression of Pol2 (**A**) and G6PD (**B**) RNA transcripts in rCD4s, obtained from infected individuals (n≥5) and treated ex vivo with a single LRA or a combination of two LRAs, presented as fold induction relative to DMSO control (mean ± s.e.m). Numbers in parentheses in Fig. 1A indicate number of individuals used for each treatment.

Supplementary Materials

Drug combinations that synergistically reverse HIV-1 latency *ex vivo* to levels approaching that of maximal T cell activation

Gregory M. Laird[†,1], C. Korin Bullen[†,1], Daniel I. S. Rosenbloom[2], Alyssa R. Martin[3], Alison L. Hill[4], Christine M. Durand[1], Janet D. Siliciano[1], and Robert F. Siliciano[1,5,*]

[1]Department of Medicine, Johns Hopkins University School of Medicine, Baltimore, MD 21205
[2]Department of Biomedical Informatics, Columbia University Medical Center, New York, NY 10032, USA
[3]Department of Pharmacology and Molecular Sciences, Johns Hopkins University School of Medicine, Baltimore, MD 21205
[4]Program for Evolutionary Dynamics, Harvard University, Cambridge, MA 02138, USA
[5]Howard Hughes Medical Institute, Baltimore, MD 21205, USA

[†]These authors contributed equally to this work
[*]To whom correspondence should be addressed; Miller Research Building, Suite 871, 733 N. Broadway, Baltimore MD 21205. Phone: 410-955-2958 Email: rsiliciano@jhmi.edu

1   Mathematical model of viral dynamics

A system of differential equations was used to describe *in vivo* viral dynamics during administration of LRA therapy, assuming that co-administered ART suppresses all viral replication. Let z be the abundance of latently infected resting CD4$^+$ T cells, let y be the abundance of activated infected CD4$^+$ T cells, and let y' be the abundance of LRA-stimulated infected CD4$^+$ T cells that are induced to produce virus, though they may not be functionally activated. Here, activation includes any LRA-independent transition to virus production, such as that caused by stochastic transcriptional changes or by antigenic stimulus. Let v be the plasma viral load, in copies per mL (c mL^{-1}). Since our conclusions will rely only on observed viral load, arbitrary units can be used for the cellular quantities. During fully suppressive ART, viral dynamics can be described by the system,

$$\dot{z} = -(a + a' + d_z)z$$
$$\dot{y} = az - d_y y$$
$$\dot{y}' = a'z - d_y' y' \tag{S1}$$
$$\dot{v} = ky + k'y' - d_v v.$$

Here, a and a' are the rates of activation and LRA-driven induction, respectively. Latently infected cells die at rate d_z. To represent the baseline (untreated) rate of reservoir decay due to combined effects of activation and death, we will use the compound parameter $\delta = a + d_z$. Activated cells produce virus at rate k and die at rate d_y; LRA-induced cells produce virus at rate k' and die at rate d_y'. Since induction is likely not as drastic as functional T cell activation, it is likely for d_y' and k' to be less than d_y and k, respectively [1]. Virus is cleared at rate d_v. The values of a', k', and d_y' depend on the LRA treatment given. The binary "switch" between latency and (either form of) activity is an idealization; it is possible that transient viral production occurs in cells experiencing varying degrees of latency.

The effect of LRA can be detected by the transient increase in viral load that it causes. To estimate this increase, we rely on observations of the *ex vivo* system. Specifically, we assume that this system also follows the above viral dynamics, with abundance of extracellular mRNA taking the place of plasma viral load for variable v. We assume moreover that parameter values are the same *in vivo* as *ex vivo*, with the exception that d_v is zero *ex vivo*. See Table S1 for discussion of these assumptions.

Generally, we assume $d_y \geq d_y'$ and that both of these cell death rates are much larger than, a, a', and d_z. Below we state explicitly where these assumptions are used.

2   Analysis of *ex vivo* dynamics

Following the above discussion, we assume $d_v = 0$. The assay begins with only resting CD4$^+$ T cells, implying initial condition $v(0) = y(0) = y'(0) = 0$ and $z(0) = z_0$, where z_0 is the number of latently infected cells collected from the cell donor (a small fraction of the 5 million cells). Since $d_v = 0$, the virus simply accumulates over time. The DMSO control provides no inducing effect beyond the baseline rate a, and the solution of system (S1) for this case is

$$v_{DMSO}(t_a) = \frac{akz_0}{d_y \delta (d_y - \delta)} \left(d_y \left(1 - e^{-\delta t_a} \right) - \delta \left(1 - e^{-d_y t_a} \right) \right), \tag{S2}$$

where the subscript in t_a indicates time in the assay, which will later be distinguished from time *in vivo*. Adding treatment applies a non-zero a'. The amount of extracellular mRNA is therefore increased by a factor:

$$\frac{v_{LRA}(t_a)}{v_{DMSO}(t_a)} \approx 1 + \frac{a'k'}{ak} \left(1 + \frac{t_a}{3} \left(d_y - d_y' - a' - ak/k' \right) \right). \tag{S3}$$

This approximation holds for $\delta t_a \ll 1$ and $\frac{t_a}{3} \left(d_y - d_y' - a' - ak/k' \right)$ near to or less than one; both are expected as $t_a \leq 1$ day in the assay, δ is the slow rate of reservoir decay (half-life of many months), and the other rate parameters are no more than 1 day^{-1}. Let ρ be the

Param.	Parameter Description	Why assumed same *ex* & *in vivo*	Caveats
a	Activation rate	Stochastic factors governing viral transcription launch a program of viral production [2]; these intracellular fluctuations may be similar in both settings.	Immune-activating effects (MHC class II presentation, cytokine signaling) not present in the assay may cause the *in vivo* value to exceed the *ex vivo* value.
a'	LRA-driven induction rate	Assay treatment conditions replicate the *in vivo* drug environment. Mechanisms causing induction are believed to rely on the same cellular transcriptional machinery in both settings.	Immune-activating effects not present in the assay may interact with the LRA effect, causing the *in vivo* value to differ from the *ex vivo* value.
k (k')	Rate of viral production by activated (LRA-induced) cells	Viral production occurs intracellularly, and primary CD4$^+$ T cells studied in the assay are a close representation of intracellular activity *in vivo*.	Cytokine production by CD8$^+$ T cells *in vivo* may suppress viral production compared to *ex vivo* rates.
d_y (d'_y)	Death rate of activated (LRA-induced) cells	Production of cytotoxic viral proteins is a major cause of cell death and may be similar in both settings (see parameters k, k' above).	CTL response, not present in the assay, may alter d_y (d'_y) *in vivo*, but see [3, 4] for evidence that this generally is not the case; also see [5] for evidence that HIV-specific responses are generally weak in HIV-infected individuals.
d_z	Death rate of latently infected cells	Low levels of transcription and viral production in latently infected cells enable long cell lifespan *ex vivo* as *in vivo*.	Conditions in the assay may not be conducive to very long cellular lifespans. Even if this parameter differs between the two settings, decay over the short duration of the assay is not expected to have a large effect on observed viral production, as noted in discussion of Eq. (S3).
Param.	Parameter Description	Why assumed zero *ex vivo*	Caveats
d_v	Viral decay rate	Viral clearance occurs primarily in lymphoid and other organs [6].	Some decay of viability of virus particles may also occur over the course of the day-long assay, at a rate slower than *in vivo*.

Table S1: Assumptions regarding comparison of *in vivo* and *ex vivo* parameters

observed value of $\frac{v_{LRA}(t_a)}{v_{DMSO}(t_a)}$ at the end of the assay. From this observation, we can estimate the following parameter ratio:

$$\frac{k'}{k} \approx \left(\frac{a}{a'}\right)\left(\frac{3(\rho - 1) + t_a a'}{3 - t_a\left(a' + d_y - d'_y\right)}\right). \tag{S4}$$

This parameter ratio estimate is used to predict viral load *in vivo*, below.

3   Analysis of *in vivo* dynamics

Since virus is subject to rapid decay *in vivo*, we can treat it using the commonly used quasi-steady state approximation: $v(t) = (ky(t) + k'y'(t))/d_v$ [7]. Likewise, since death rate d_y greatly exceeds baseline activation rate a, the initial number of actively infected cells can be approximated by activation-death equilibrium, $y(0) = az_0/d_y$, implying a residual viral load of $v(0) = akz_0/(d_yd_v)$. The fractional increase in viral load caused by administering the LRA for a period of time t follows from these assumptions and system (S1):

$$
\begin{aligned}
\frac{v_{LRA}(t)}{v(0)} &= \frac{d_y e^{-(\delta+a')t} - (\delta+a')e^{-d_y t}}{d_y - \delta - a'} \\
&\quad + \frac{d_y\left(3(\rho-1)+a't_a\right)\left(e^{-(\delta+a')t} - e^{-d'_y t}\right)}{\left(d'_y - \delta - a'\right)\left(3 + t_a\left(d_y - d'_y - a'\right)\right)}.
\end{aligned}
\tag{S5}
$$

Here, eq. (S4) has been used to eliminate both k and k' by introducing the *ex vivo*-observed parameter ρ. The first line of (S5) represents viremia due to activated cells, while the second line represents viremia due to LRA-induced cells.

The *in vivo* viral load ratio in (S5) approximates a bi-exponential curve, initially rising linearly from 1 at rate $\approx d_y(\rho-1)$ and ultimately decaying exponentially at rate $\delta + a'$. The maximum value cannot be expressed in a simple form, but the peak viral load ratio can be approximated by noting that the first line of (S5) falls between 0 and 1, while the second line (for which the maximum can be expressed in closed form) has a peak much larger than 1 for typical parameter values ($d_y \geq d'_y > a' > \delta$, none of these rates much larger than 1 day^{-1}, and $\rho \gg 1$). The peak viral load, relative to the baseline residual viral load, is therefore approximately

$$
\frac{\max\left(v_{LRA}(t)\right)}{v(0)} \lesssim 1 + \left(\frac{d_y}{d'_y}\right)(3(\rho-1)+a't_a)\left(\frac{\left(\frac{\delta+a'}{d'_y}\right)^{\frac{\delta+a'}{d'_y - \delta - a'}}}{3 + t_a\left(d_y - d'_y - a'\right)}\right),
\tag{S6}
$$

and it occurs approximately at time

$$
t_{\max} \approx \frac{\ln\left(d'_y/(\delta+a')\right)}{d'_y - \delta - a'}.
\tag{S7}
$$

The approximation in Eq. (S6) never overestimates the true peak ratio by more than 1. Note that the exponentiated expression decreases with the sum $(\delta + a')$, indicating the effect of a rapidly decaying reservoir on the peak viral load. If $(\delta + a')$ is very small relative to d'_y, then the peak viral load is simply

$$
\frac{\max\left(v_{LRA}(t)\right)}{v(0)} \lesssim 1 + (\rho - 1)\frac{d_y}{d'_y}.
\tag{S8}
$$

This approximation is used in Fig. 7B. Note that this result does not depend on the LRA-driven induction rate a' nor the viral production rate k' of LRA-induced cells; the experimentally observed parameter ρ depends on a combination of induction and production. Further

experiments — involving measurement of the fraction of cells induced or the decay in viral production over time — would be needed to resolve rate a', which determines the rate at which LRA therapy would ultimately deplete the latent reservoir.

4   *In vivo* dynamics for short treatment window

The previous section assumes that treatment is administered continuously, until the latent reservoir eventually decays completely, yet such a regimen may not be achievable. Suppose instead that the effect of treatment ceases at time t_{Stop}, after which point a' is set to zero. For $t > t_{Stop}$, the viral load ratio is:

$$
\begin{aligned}
\frac{v_{LRA}(t)}{v(0)} &= \frac{e^{-(d_y+\delta)t-(\delta+a')t_{Stop}}}{(d_y-\delta)(d_y-\delta-a')} \\
&\quad \times \Bigg[d_y^2 e^{d_y t+\delta t_{Stop}} - d_y \left((\delta+a') \left(e^{d_y t+\delta t_{Stop}} + e^{\delta t+(\delta+a')t_{Stop}} \right) - a' e^{\delta t+d_y t_{Stop}} \right) \\
&\quad + \delta(\delta+a') e^{\delta t+(\delta+a')t_{Stop}} \Bigg] \\
&\quad + e^{-d_y'(t-t_{Stop})} \frac{d_y \left(3(\rho-1)+a't_a\right) \left(e^{-(\delta+a')t_{Stop}} - e^{-d_y' t_{Stop}} \right)}{\left(d_y'-\delta-a'\right)\left(3+t_a\left(d_y-a'-d_y'\right)\right)}.
\end{aligned}
\tag{S9}
$$

As in Eq. (S5), the first term (spanning the first three lines) represents the portion due to activated cells, while the second term (on the final line) represents the portion due to LRA-induced cells. This expression is used to compute the curves in Figs. 7C and 7D. Note that this dynamic treats the LRA as pharmacologically active at maximum concentration at the start of therapy; a more realistic model would include an absorption phase during which viral load may increase more gradually.

5   Parameters used in Fig. 7

For each treatment described in Fig. 7B, ρ was chosen to match the median value observed in the *ex vivo* assay, given in Table S2. To provide viral load estimates, pre-treatment residual viremia of 2 c ml^{-1} was used. Eq. (S8) was used to compute peak viral load, with d_y/d_y' of 1 or 3.

For Figs. 7C and 7D, Eq. (S9) was used, and both ρ and pre-treatment residual viremia were as in Fig. 7B. Baseline activation rate $a = 5.7 \times 10^{-5}$ day^{-1} and latent cell death rate $d_z = 4.66 \times 10^{-4}$ day^{-1} were chosen to be consistent with observed residual viremia and reservoir half-life of 44 months [8]. Death rate d_y was set to 1 day^{-1} [9], and d_y' was either 1 day^{-1} (blue curves) or 1/3 days $^{-1}$ (red curves). For blue curves, a' for each treatment was chosen using the relationship (S4), assuming $d_y/d_y' = k/k' = 1$ (see Table S2). For red curves displaying romidepsin treatment, a' of 0.002 day^{-1} was chosen to be consistent with $d_y/d_y' = k/k' = 3$.

Treatment	ρ	a' (day^{-1})
Romidepsin	15	8.0×10^{-4}
Prostratin + romidepsin	104	0.0059
Bryostatin-1 + romidepsin	105	0.0059
Bryostatin-1	120	0.0068
Prostratin	209	0.012
Prostratin + JQ1	297	0.017
Bryostatin-1 + JQ1	401	0.023
PMA + ionomycin	554	0.032

Table S2: Treatment-specific parameters used for blue curves in Figs. 7C and 7D

References

[1] L. Shan, *et al.*, *Journal of Antimicrobial Chemotherapy* **69**, 28 (2014).

[2] A. Singh, L. S. Weinberger, *Current Opinion in Microbiology* **12**, 460 (2009).

[3] N. R. Klatt, *et al.*, *PLoS pathogens* **6**, e1000747 (2010).

[4] J. K. Wong, *et al.*, *PLoS pathogens* **6**, e1000748 (2010).

[5] L. Shan, *et al.*, *Immunity* **36**, 491 (2012).

[6] L. Zhang, P. J. Dailey, A. Gettie, J. Blanchard, D. D. Ho, *Journal of virology* **76**, 5271 (2002).

[7] A. S. Perelson, A. U. Neumann, M. Markowitz, J. M. Leonard, D. D. Ho, *Science* **271**, 1582 (1996).

[8] A. L. Hill, D. I. S. Rosenbloom, F. Fu, M. A. Nowak, R. F. Siliciano, *Proc. Natl. Acad. Sci. USA* (Online ahead of print, Aug. 5, 2014).

[9] M. Markowitz, *et al.*, *Journal of virology* **77**, 5037 (2003).